Enhancing DNA-Based IoBNT Throughput and Reducing Congestion with Yin-Yang Coding

Wanli Cheng[1], Yue Sun[1(✉)], Qingwen Wang[1], Yifan Chen[2], and Kun Yang[3]

[1] The School of Mechanical and Electrical Engineering, Chengdu University of Technology, Chengdu 610059, China
sunyuestc90@126.com
[2] The School of Life Science and Technology, University of Electronic Science and Technology of China, Chengdu 610000, China
[3] University of Essex, Colchester CO4 3SQ, U.K.

Abstract. This paper presents a focused analysis of enhancing the Internet of Bio-Nano Things (IoBNT) network performance by addressing congestion and improving throughput. We introduce a propagation model for a high-throughput DNA-based track-hopper channel to study congestion using molecular hopper dynamics and Markov state transitions alongside a novel approach for throughput measurement. Our research aims at reducing congestion by increasing information density, allowing for more efficient data transmission with fewer packets. Initially, attempts to amplify density encountered challenges related to bio-compatibility and increased decoding errors. Moreover, congestion precipitated the formation of problematic DNA structures such as hairpins during sequencing. We adopted the yin-yang coding (YYC) to overcome these hurdles, encoding two binary bits into one nucleotide for sequences compatible with synthesis and sequencing technologies. Simulation results validate the YYC coding mechanism's effectiveness and propagation models' robustness, significantly advancing IoBNT network performance optimization.

Keywords: IoBNT · Molecular Hopper · Markov State Transition · Network Congestion · Network Throughput

1 Introduction

The Internet of Bio-Nano Things (IoBNT) embodies an innovative fusion of biology, nanotechnology, and information communication technologies, heralding a new era of integration across these domains. This interdisciplinary approach

This work is supported by the National Natural Science Foundation of China (Grants No. 62301088).

Y. Chen et al. (Eds.): BICT 2024, LNICST 592, pp. 20–31, 2025.
https://doi.org/10.1007/978-3-031-81599-7_3

seeks to replicate and augment the complex network interactions found in natural systems using nanoscale sensors and nanorobots [1]. The ultimate aim is to construct a network of microscopic entities capable of performing sensing, processing, and actuation tasks—thereby extending the functionalities of the traditional Internet of Things (IoT) to the nanoscale domain [2].

Building on the foundational work introducing a novel IoBNT framework utilizing track-hopper-based DNA molecular communication(DNA-MC), we have previously demonstrated how DNA's inherent properties can facilitate robust intra- and extra-body communication [3]. By adopting a mesh network topology over traditional tree-like structures, our designs have enhanced fault tolerance and network resilience, ensuring reliable connectivity among nodes and safeguarding against disruptions. In advancing this domain, our current research delves into the critical issue of network congestion within the IoBNT, aiming to identify and mitigate congestion scenarios to improve system stability and performance metrics, such as low delay and high throughput, as discussed in [4]. Our novel approach employs the yin-yang coding (YYC) mechanism to enhance information density, facilitating more efficient data transmission and addressing bio-compatibility and decoding accuracy challenges [5]. This coding strategy mitigates the formation of problematic DNA structures, such as hairpins, and ensures compatibility with synthesis and sequencing technologies, marking a significant leap in addressing IoBNT network congestion.

We aim to provide a comprehensive understanding of how our integrated solutions—particularly the yin-yang coding scheme—significantly enhance the efficiency and reliability of the IoBNT framework, offering novel insights into overcoming the challenges of congestion and throughput in bio-nano networks.

This paper is structured as follows: Sect. 2 introduces our models for analyzing network congestion levels, including molecular hopper dynamics and Markov state transitions. Section 3 details the yin-yang coding mechanism and its impact on network throughput. Section 4 discusses our simulation setup and the empirical validation of our models, and Sect. 5 synthesizes our main findings and concludes the paper.

2 Network Congestion Degree Modeling

2.1 Molecular Hopper Transmission Dynamics Model

To effectively model congestion levels within the IoBNT network, it is essential first to ascertain the rates of individual links during the information transmission. Drawing inspiration from the vehicular traffic queuing models, which analyze the flow of cars on road networks, our approach introduces a molecular hopper transmission queuing dynamics model specific to our IoBNT framework [6]. This innovative model adopts the protein track utilization rate as a pivotal dynamic variable, offering a detailed mechanism to understand the operations of the track-hopper system. By adjusting the length of the protein track, we can establish a comprehensive and unified scheme for modeling the state of information transmission across the network. Consider a protein track denoted as i and

the utilization rate of it is dynamically influenced by the number of molecular hoppers present, thereby providing a nuanced view of the system's congestion dynamics at the molecular level. We first analyze the utilization of a single hopper on the track:

$$\alpha_i = \frac{l_{sd}}{l_i} \tag{1}$$

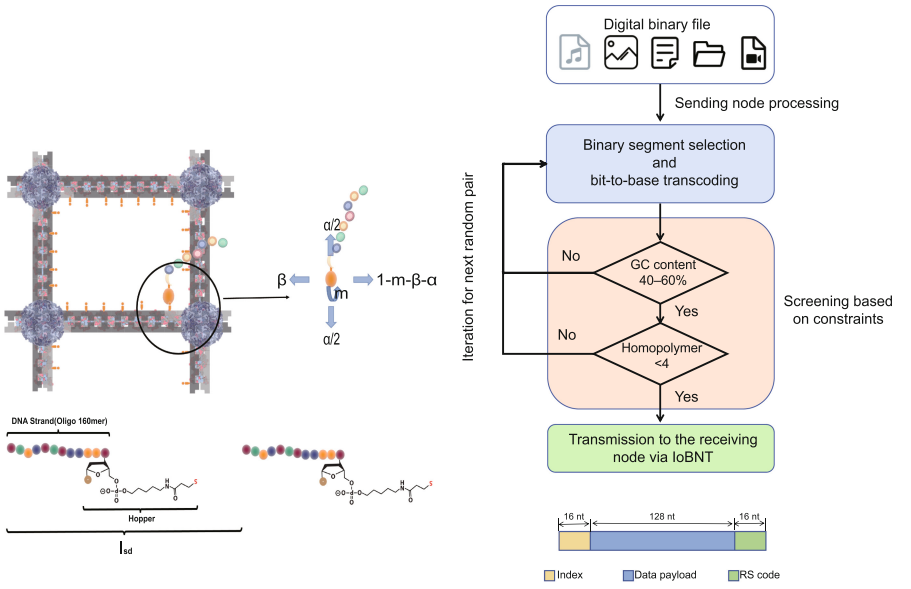

(a) (b)

Fig. 1. (a)The motion-state probability model of the molecular hopper is shown. (b)Shows a safe distance l_{sd}.

In the formulas, where α_i represents the utilization rate of a single hopper on the track. l_i denotes the length of track i, l_{sd} represents the distance between adjacent molecular hoppers carrying DNA sequences (indicating a safety distance, defined as the potential for hoppers to retreat during the transportation process considering the occurrence of two retreat events, and as the DNA sequences carried by the hoppers are fixed, l_{sd} is defined as the sum of the DNA sequence length, hopper length, and the safety distances for the two possible retreat events).

Subsequently, we extend our analysis to examine the track utilization of multiple molecular hoppers.

$$U_i\left(t\right) = \alpha_i R_i\left(t\right) \tag{2}$$

where $U_i\left(t\right)$ represents the utilization rate of track i at time step t, $R_i\left(t\right)$ represents the number of hoppers on track i at time step t.

Building upon the previously established definitions, the actual count of hoppers conveyed along track i at the specific time step t can be accurately calculated:

$$O_i(t) = min(R_i(t), X_i(t)) \tag{3}$$

$$X_i(t) = \frac{T}{h_{min}} \tag{4}$$

where $O_i(t)$ represent the number of hoppers leaving track i during the time interval $[tT, (t+1)T]$. $X_i(t)$ represents the number of hoppers processed and completed at the end node of track i during the time interval t. h_{min} represents the time difference between the processing of two consecutive hoppers at the node, which can be calculated by adding the processing time for the DNA sequences at the node and the time for forwarding the information. T represents the total processing time interval.

Combining the concepts discussed previously, we can derive the relationship between the track i at time step $(t+1)$ and its utilization at time t.

$$U_i(t+1) - U_i(t) = \alpha_i [I_i(t) - O_i(t)] \tag{5}$$

let $I_i(t)$ denote the number of hoppers entering track i during the time interval $[tT, (t+1)T]$. The definitions and implications of other parameters are detailed in Eqs. (1), (2), (3), and (4). This enables us to grasp the influence of a track's current utilization on its future condition, offering valuable insights into its temporal dynamics and furnishing a thorough framework for comprehending the system's behavior over time.

According to the description in [7], suppose a molecular hopper enters track i correctly with probability p and turns to enter the wrong track with probability $(1-p)$. In n time steps, the number of hoppers M correctly entering track i follows a binomial distribution, i.e., $M \sim \mathcal{B}(n, p)$. Therefore, for large n and np, the number of hoppers correctly entering track i can be approximated by Poisson $\mathcal{P}(\lambda)$ distribution. Thus, the probability of m hoppers reaching track i in the interval $[tT, (t+1)T]$ can be calculated as:

$$P(I_i(t) = m) = \frac{\lambda_i(t)^m \cdot e^{-\lambda_i(t)}}{m!} \tag{6}$$

where $\lambda_i(t)$ represents the expected arrival rate at track i for each time interval T at time step t, which is determined based on the network topology shown in Fig. 1(a). In Fig. 1(a), β represents the probability of the hopper moving backward, m represents the probability of the hopper remaining stationary, and $\frac{\alpha}{2}$ represents the probability of the hopper transmitting information in the wrong direction. By considering the characteristics of the dual-path network topology, we ultimately obtain the expected arrival rate at each time interval T for track i at time step t: $2 \cdot (1 - m - \beta - \alpha)$.

2.2 Markov State Transition Model

In this section, we have modeled the transition of track occupancy states and obtained the Markov state transition matrix for track occupancy states. In this

paper, we categorize track occupancy states into three levels: 1: indicating the absence of congestion and a good track state; 2: indicating moderate congestion; 3: indicating severe congestion. Thus, we can derive the discretization formula for the state of track i as follows:

$$s_i(t) = \begin{cases} 1 & 0 \le U_i(t) < a \\ 2 & a \le U_i(t) < b \\ 3 & b \le U_i(t) \le 1 \end{cases} \tag{7}$$

where a and b represent the corresponding track utilization rates. For the three states, the track utilization rate $U_i(t)$ follows a discrete uniform distribution with two parameters (upper and lower bounds).

Based on the expression of the state of track i as described above, it is known that there are 9 possible events that may occur during each time interval T, and the probability of each event occurring is different. By considering the expected arrival rate $\lambda_i(t)$ and the node processing time t_p at time step t, a Markov state transition matrix can be derived to describe the congestion level of track i:

$$P_i(t) = \begin{bmatrix} {p_i}^{11}(t) & {p_i}^{12}(t) & {p_i}^{13}(t) \\ {p_i}^{21}(t) & {p_i}^{22}(t) & {p_i}^{23}(t) \\ {p_i}^{31}(t) & {p_i}^{32}(t) & {p_i}^{33}(t) \end{bmatrix} \tag{8}$$

where, the probability of each state transition is defined as:

$${p_i}^{mn}(t) = Pr\left(s_i(t+1) = n \mid s_i(t) = m\right) \tag{9}$$

among $m, n = 1, 2, 3$, due to the complexity of the derivation process, in this section we only discuss ${p_i}^{11}(t)$, and the rest of the matrix elements are similar.

By the definition of each state transition probability, we can obtain that ${p_i}^{11}(t)$ represents the probability of the state $s_i(t)$ being restricted to 1 and the state $s_i(t+1)$ also being 1. When $\alpha_i \cdot X_i(t)$ is greater than a, we can obtain $U_i(t+1) = \alpha_i I_i(t)$, according to (2), (3), (4), (5) and (6). Therefore, we can obtain the value of ${p_i}^{11}(t)$ as:

$${p_i}^{11}(t) = \sum_{n=1}^{floor(a/\alpha_i)} \frac{\lambda_i(t)^n \cdot e^{-\lambda_i(t)}}{n!} \tag{10}$$

where $floor(x)$ refers to the largest integer that is less than or equal to x.

When $\alpha_i \cdot X_i(t)$ is less than a, we can obtain the representation of $U_i(t+1)$ as:

$$U_i(t+1) = \begin{cases} \alpha_i I_i(t) & 0 \le U_i(t) < \alpha_i \cdot X_i(t) < a \\ U_i(t) + \alpha_i I_i(t) - \alpha_i \cdot X_i(t) & 0 \le \alpha_i \cdot X_i(t) < U_i(t) < a \end{cases} \tag{11}$$

According to the law of total probability, we can obtain the final expression for ${p_i}^{11}(t)$:

$$\begin{aligned} {p_i}^{11}(t) = {} & Pr\left(s_i(t+1) \mid U_i(t) \in [0, \alpha_i \cdot X_i(t))\right) \\ & \cdot Pr\left(U_i(t) \in [0, \alpha_i \cdot X_i(t))\right) \\ & + Pr\left(s_i(t+1) \mid U_i(t) \in [\alpha_i \cdot X_i(t), a)\right) \\ & \cdot Pr\left(U_i(t) \in [\alpha_i \cdot X_i(t), a)\right) \end{aligned} \tag{12}$$

According to (2), (3), (4), (5) and (6), the final expression for ${p_i}^{11}(t)$ can be derived as follows:

$$\begin{aligned} {p_i}^{11}(t) = & \frac{\alpha_i X_i(t)}{a} \sum_{n=1}^{floor(a/\alpha_i)} \frac{\lambda_i(t)^n \cdot e^{-\lambda_i(t)}}{n!} \\ & + \frac{a - \alpha_i X_i(t)}{a\left(y - X_i(t)\right)} \sum_{n=X_i(t)}^{y+X_i(t)} \sum_{i=X_i(t)}^{min(n,y)} \frac{\lambda_i(t)^{n-i} \cdot e^{-\lambda_i(t)}}{(n-i)!} \end{aligned} \tag{13}$$

with $y = floor\left(a/\alpha_i\right)$.

Based on the derived formula, we can further obtain the average value of $R_i(t+1)$ in this state:

$$\overline{R}_i{}^{11}(t+1) = \frac{1}{\alpha_i} \sum_{n=0}^{y} U_i(t+1)\, Pr\left(U_i(t+1) = n\alpha_i\right) \tag{14}$$

$$Pr\left(U_i(t+1) = n\alpha_i\right) = Pr\left(U_i(t) + \alpha_i\left[I_i(t) - O_i(t)\right] = n\alpha_i\right) \tag{15}$$

Hence, in a similar manner, the average number of molecular hoppers corresponding to each transition state can be obtained for the state transitions occurring in each orbit:

$$\overline{R}_i(t+1) = \begin{bmatrix} \overline{R}_i{}^{11}(t+1) & \overline{R}_i{}^{12}(t+1) & \overline{R}_i{}^{13}(t+1) \\ \overline{R}_i{}^{21}(t+1) & \overline{R}_i{}^{22}(t+1) & \overline{R}_i{}^{23}(t+1) \\ \overline{R}_i{}^{31}(t+1) & \overline{R}_i{}^{32}(t+1) & \overline{R}_i{}^{33}(t+1) \end{bmatrix} \tag{16}$$

Furthermore, when the current state of the track is known, the average number of hoppers transferred through track i at time $(t+1)$ with the same congestion level as time t can be calculated by the $\overline{R}_i{}^{mn}(t+1)$:

$$\overline{R}_i{}^{m}(t+1) = \sum_{n=1}^{3} \overline{R}_i{}^{mn}(t+1)\, {p_i}^{mn}(t) \tag{17}$$

where $m, n = 1, 2, 3$. Thus, we have obtained the Markov state transition matrix for the network topology, which is updated comprehensively based on the time-varying information flow and node processing time for each link. Furthermore, based on the obtained matrix of average hopper quantities corresponding to each transition state, we can calculate the maximum information flow that each link can sustain to maintain the current state.

Once $\overline{R}_i{}^{m}(t+1)$ has been obtained, according to (4) and (5), we can determine the number of hoppers arriving at the receiving node for link i in state m during the time interval $(t+1)$. This quantity corresponds to the number of output packets for the given conditions:

$$\overline{O}_i{}^{m}(t+1) = min\left(\overline{R}_i{}^{m}(t+1), \frac{T}{h_{min}}\right) \tag{18}$$

3 DNA Coding Scheme and Network Throughput Model

3.1 Yin-Yang Coding

Over the past decade, the rapid development of gene synthesis and sequencing technologies has highlighted the favorable characteristics of DNA messenger molecules as information carriers. These factors include stability, information longevity, high information density, large-scale parallelism, and biocompatibility, making DNA one of the best choices as an information carrier in IoBNT systems [8]. However, due to the limitations of current DNA synthesis technology, the de novo synthesis of long DNA sequences remains challenging. When transmitting large amounts of information using IoBNT, it is necessary to decompose the long DNA sequences formed by encoding binary information into smaller fragments (150 ∽ 200 bases) [9]. In the previous section, we proposed a model of network congestion levels to calculate the average number of hoppers transmitted through link i under each congestion level. Excessive hoppers transmitting information on the same link can cause network congestion, potentially leading to the paralysis of local networks. Therefore, a robust DNA encoding method is needed to compress the information to be transmitted into fewer DNA data packets, while ensuring the integrity and accuracy of the information when decoded at the receiver. Figure 2 shows the coding rules and procedure for YYC in detail.

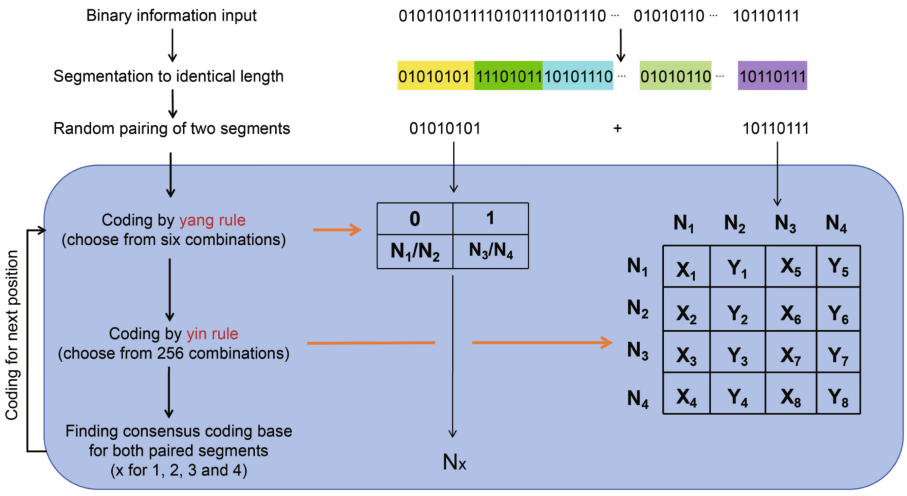

Fig. 2. The bit-to-base transcoding process of the YYC.

The YYC algorithm, proposed by Ping Zhi et al. in 2022, is a coding scheme for DNA-based data archiving [10]. YYC draws inspiration from the traditional Chinese concept of Yin and Yang, representing two distinct yet complementary and interdependent principles.

Table 1. Comparison of DNA-based coding schemes

General attributes	Church et al.	Goldman et al.	Grass et al.	Erlich et al.	Chen et al.	YYC
Error correction strategy	No	Repetition	RS	Fountain	LDPC	RS
Robustness against errors	Yes	Yes	Yes	No	Yes	Yes
Information density	1	1.58	1.78	1.98	1.24	1.95
GC content of sequences	2.5–100	22.5–82.5	12.5–100	40–60	N/A	40–60
Maximum homopolymer length	3	1	3	4	N/A	4

The YYC algorithm merges two independent coding rules, "yin" and "yang" into a single DNA sequence, compressing two nucleotides into one. Using N_1, N_2, N_3, and N_4 to represent the nucleic acids A, T, C, G, respectively, the Yang rule generates six coding combinations, while the yin rule maps N_1/N_2 and N_3/N_4 to independent binary numbers, resulting in 256 coding combinations. The merged yin-yang rule provides a total of 1536 (6×256) transcoding scheme combinations for encoding binary sequences, ensuring consistent nucleotide generation and independent options for the previous nucleotide.

Subsequent simulations and experiments have shown that the YYC method effectively eliminates the formation of long homopolymer sequences, while keeping the GC content of the produced DNA sequences within a desirable range of 40% to 60%. Unlike other coding approaches that rely on fixed mapping rules, YYC employs dynamic combinatorial coding schemes. It leverages the Yin and Yang rules to create a total of 1536 encoding schemes, tailored for various data types. This flexibility enables the generation of optimal DNA sequences, overcoming challenges in DNA synthesis and sequencing, such as those associated with long homopolymers and extreme GC contents. Additionally, YYC exhibits a higher information density, meaning that more bits of information can be represented per DNA base compared to other schemes. This results in the ability to represent the same data set with fewer DNA sequences.

Table 1 provides a comparison of various coding schemes based on DNA. It is evident that the information density of YYC is higher compared to most DNA coding schemes, with only a slight difference of 0.03 $bits\ nt^{-1}$ from DNA Fountain, which falls within an acceptable range. Additionally, YYC demonstrates superior control over GC content and maximum average polymer length compared to other coding schemes.

Considering the robust information density and error correction capabilities of YYC, we have selected it as the coding scheme for the IoBNT system proposed in our study. Figure 1(b) depicts the comprehensive process diagram of the system utilizing YYC for encoding.

3.2 Network Throughput Model

Building upon the definition of wireless network throughput as described in [11], we have established and computed the network throughput for the IoBNT

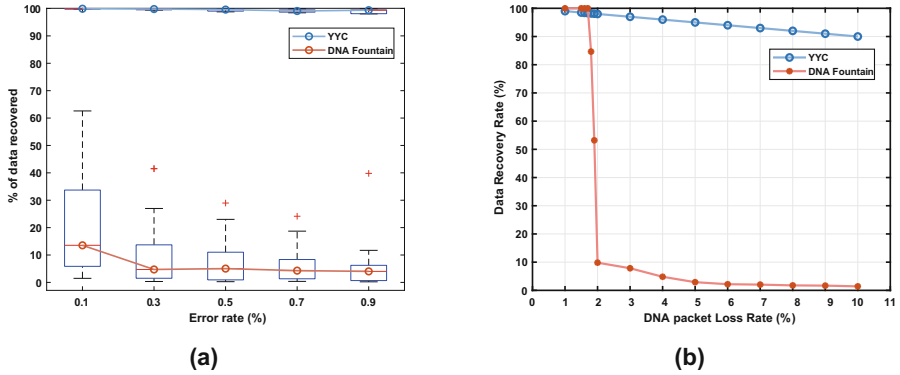

Fig. 3. Performance comparison of YYC and DNA Fountain. (a)Robustness analysis for the YYC and DNA Fountain coding schemes. (b)The simulation of the data recovery rate in the context of a gradient of DNA sequence loss.

system that we propose. Based on the information density of YYC described in Table 1 and the DNA sequences designed and generated by YYC in Fig. 1(b), we can calculate that each DNA data packet carries approximately 250 bits of information. According to (17), we can determine the number of data packets output by link i at time $(t+1)$. Therefore, based on the above information, we can calculate the total amount of information output at time $(t+1)$:

$$M = 250 \cdot \overline{O}_i^{\,m}(t+1) \tag{19}$$

Therefore, we can obtain the network throughput as:

$$H = \frac{M}{T_z} \tag{20}$$

where, $T_z = T_t + T_d$.

$$T_t = \frac{l}{v\Lambda} \frac{\sqrt{D^2 + V^2 x^2} - D}{V^2}, \tag{21}$$

$$T_d = \frac{\overline{O}_i^{\,m}(t+1) \cdot 160 \cdot 0.34}{v}, \tag{22}$$

where T_t is the DNA sequence transmission time, T_d is the time it takes for the DNA sequence to be decoded at the receiver, l is the target length of the molecular hopper movement,x is the length of the link and v is the forward velocity of the molecular hopper movement. D is the diffusion coefficient, V is the drift coefficient, and Λ is the reaction coefficient; the calculation of these parameters, we have given in [3]. 160 nt is the number of bases per DNA packet, and 0.34 is the length of each base of 0.34 nm [12].

4 Simulation and Results

Figure 3(a) illustrates that Robustness analysis for the YYC and DNA Fountain coding schemes. The boxplot comparison between YYC and DNA Fountain

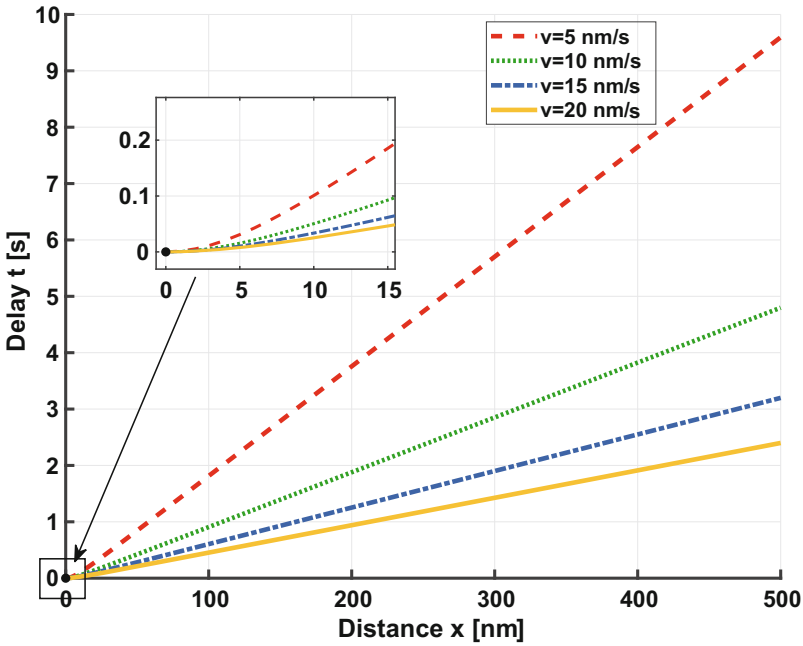

Fig. 4. System delay vs distance for different v datas.

illustrates that while both methods perform comparably well at low error rates, YYC demonstrates superior consistency and robustness, maintaining high data recovery rates even as the error rate increases. In contrast, DNA Fountain shows a decline in performance with increasing error rates, exhibiting more variability and a higher number of outliers, indicating less predictability and reliability. Overall, YYC proves to be more resilient and dependable across a wider range of error conditions. Figure 3(b) shows the performance of YYC and DNA Fountain under different DNA packet loss rates. YYC has a significantly higher data recovery rate across the entire test range compared to DNA Fountain. When the oligonucleotide loss rate is low, the recovery rate of DNA Fountain drops sharply, while YYC demonstrates stronger recovery stability, maintaining a higher recovery rate even as the loss rate increases. This suggests that YYC may be more reliable and effective in terms of data recovery.

Figure 4 presents the system delay of the IoBNT. These simulation results provide insights into the delay characteristics of the nanonetwork based on different scales of molecular hoppers, particularly at small scales ($x < 6\,nm$) and large scales ($x > 6\,nm$). This graph depicts two different relationships between delay and distance. At small scales, there exists a nonlinear relationship between delay and distance. This is because at shorter distances, the transmission delay is mainly determined by the hopper movement speed (v) and the characteristic length of the hopper (l). When the distance is short, the impact of the link

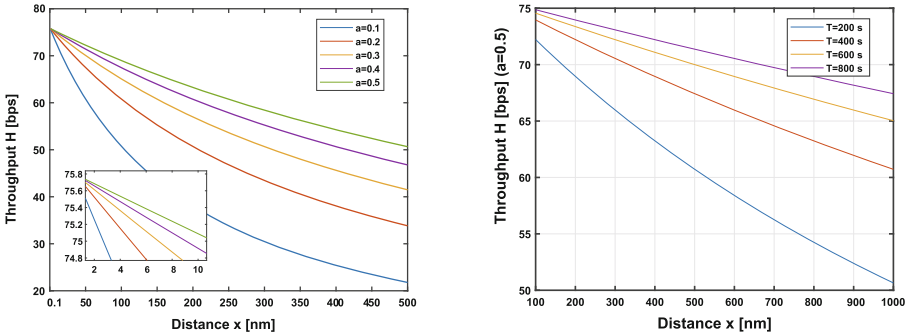

(a) (b)

Fig. 5. (a)Under different probability a network throughput with the change of link distance. (b)The impact of different processing times for information at nodes on throughput.

length on delay is relatively small, resulting in lower delay. However, as the distance increases, the effect of information transmission distance becomes more significant. After a certain point, the delay starts to increase rapidly because the information needs to be transmitted through longer links, resulting in a linear relationship between delay and distance, where the delay increases with distance.

Figure 5(a) illustrates that as the distance increases, network throughput gradually decreases. The parameter a represents the upper limit of link utilization in state 1, and different values of parameter a have varying degrees of impact on throughput. Smaller a values exhibit superior throughput sustainability in long-distance transmission, indicating that the system is more resilient to the performance degradation caused by increased distance under smaller a values. These findings are valuable for the design and optimization of long-distance transmission systems. The trend of changes in network throughput under different processing times T is shown in Fig. 5(b). As the processing time increases, the number of data packets outputted by the network also increases, resulting in a higher amount of information transmitted per unit of time, i.e., higher throughput.

5 Conclusion

In this study, we established a comprehensive network congestion model for IoBNT based on DNA MC and track-hoppers, effectively capturing the dynamics of network congestion through the development of a Markov state transition matrix and quantifying the average number of data packets per link necessary for system equilibrium. We introduced and utilized the YYC coding scheme, laying the groundwork for a sophisticated network throughput model that showcases the scheme's efficacy. Through detailed simulations, we analyzed the effects of molecular hopper speeds and transmission distances on IoBNT system delay,

highlighting the minimal impact of link length at shorter distances and the significant influence of transmission distance as it increases. Our comparison between the YYC coding scheme and DNA Fountain under varying error rates demonstrated YYC's comparable information density and superior data recovery capabilities. Furthermore, our simulations of network throughput under diverse conditions elucidated the positive correlation between throughput, link utilization ceiling, and node information processing time. Looking ahead, our future efforts will concentrate on advancing network routing algorithms, leveraging the insights gained from our network congestion model to bolster the system's robustness and reliability, thereby marking a significant step forward in the optimization of IoBNT systems.

References

1. Akyildiz, I.F., Pierobon, M., Balasubramaniam, S., Koucheryavy, Y.: The internet of Bio-Nano things. IEEE Commun. Mag. **53**(3), 32–40 (2015)
2. Malak, D., Akan, Ö.B.: Molecular communication nanonetworks inside human body. Nano Commun. Netw. **3**(1), 19–35 (2012)
3. Wang, Q., Sun, Y., Cheng, W., Chen, Y., Yang, K.: Novel interleaved code for high-throughput parallel DNA-based molecular communications. IEEE Commun. Lett. **27**(10), 2593–2597 (2023)
4. Pramanik, P.K., Solanki, A., Debnath, A., Nayyar, A., El-Sappagh, S., Kwak, K.S.: Advancing modern healthcare with nanotechnology, nanobiosensors, and internet of nano things: taxonomies, applications, architecture, and challenges. IEEE Access **8**, 65230–65266 (2020)
5. Wang, P., Mu, Z., Sun, L., Si, S., Wang, B.: Hidden addressing encoding for DNA storage. Front. Bioeng. Biotechnol. **10**, 916615 (2022)
6. Xu, Y., Xi, Y., Li, D., Zhou, Z.: Traffic signal control based on markov decision process. In: 2016 8th IFAC Conference on Manufacturing Modelling, Management and Control MIM, 28—30 June 2016 (2016)
7. Hofmann, P., Cabrera, J.A., Bassoli, R., Reisslein, M., Fitzek, F.H.: Coding in diffusion-based molecular nanonetworks: a comprehensive survey. IEEE Access **11**, 16411–16465 (2023)
8. Liu, Q., Yang, K., Xie, J., Sun, Y.: DNA-based molecular computing, storage, and communications. IEEE Internet Things J. **9**(2), 897–915 (2021)
9. Doricchi, A., et al.: Emerging approaches to DNA data storage: challenges and prospects. ACS Nano **16**(11), 17552–17571 (2022)
10. Ping, Z., et al.: Towards practical and robust DNA-based data archiving using the yin-yang codec system. Nat. Comput. Sci. **2**(4), 234–242 (2022)
11. Li, P., Fang, Y.: On the throughput capacity of heterogeneous wireless networks. IEEE Trans. Mob. Comput. **11**(12), 2073–2086 (2012)
12. Minchin, S.D., Lodge, J.F.: Understanding biochemistry: structure and function of nucleic acids. Essays Biochem. **63**(4), 433–456 (2019)